Golden Selection Search for Single Beacon Homing

Andrew Branch, James Mason, Steve Chien
Jet Propulsion Laboratory, California Institute of Technology
4800 Oak Grove Drive
Pasadena, California 91109
andrew.branch@jpl.nasa.gov

Abstract

Exploration of Ocean Worlds requires a new type of mission to be developed, an ice penetrating submersible vehicle. Such a mission would present a number of new challenges, including long range autonomous under ice navigation. We have developed a method based on Golden Section Search for an AUV to home to a base station with a single range-only acoustic beacon and no absolute heading measurement capabilities. We demonstrate this method in simulation to home from 10km away to within 1km. Such capabilities would be required for a submersible to explore any substantial portion of the oceans on these Ocean Worlds.

Introduction

Liquid oceans are thought to exist on at least eight bodies in our solar system. On all bodies except for Earth, these oceans are encased in an icy shell, potentially kilometers thick (National Aeronautics and Space Administration 2018). Ice penetrating, submersible vehicles would need to be developed to study these worlds. A notional mission concept for such a submersible contains three main components: a surface antenna, a fixed under-ice base station, and a submersible vehicle, shown in Figure 1. A cryobot would penetrate the icy shell, deploying the base station and submersible vehicle at the bottom of the borehole. The vehicle would be able to acoustically communicate to the base station which can then be relayed through the surface antenna to Earth. The long mission duration — potentially over a year to melt through the icy shell and a one year exploration mission — requires a low power vehicle, limiting the types of instruments on board. The vehicle would ideally travel hundreds of kilometers distant from the base station while being able to return to transfer data, with data subsequently relayed from the base station, through the surface antenna to Earth. When the submersible is distant from the base station, which would be required to explore a large amount of the ocean, it will be unable to communicate with Earth.

For the vehicle to travel outside of communication range with the base station it must be able to reliably return. An acoustic beacon or set of beacons on the base station would enable underwater navigation. A number of constraints drive viable underwater navigation strategies. First, acoustic sources can only be co-located with the base station. Deploying additional sources at disparate locations, either through additional boreholes or once under-ice, would significantly increase mission cost and complexity. Second, a long-range (>10 km) acoustic navigation beacon would only be capable of providing range measurements to the vehicle. Finally, due to the time-varying induced magnetic field of Ocean Worlds such as Europa, we assume that no absolute heading measurements via magnetic navigation is possible. We present a homing method that will allow the vehicle to return to the base station while using only a single acoustic beacon with range-only capabilities and an IMU with no absolute heading information.

The remainder of the paper is organized as follows. We present related works, our homing method, the simulated experiment, and the results. Finally we discuss the results and present future work.

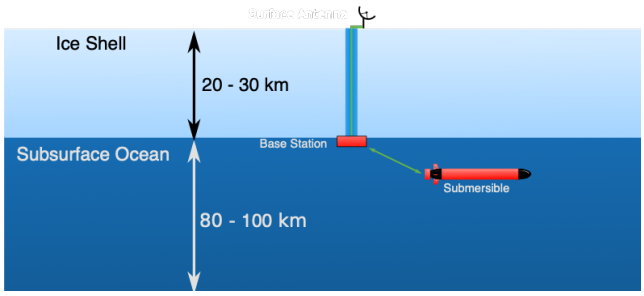

Figure 1: Diagram of a concept Ocean Worlds submersible. Three main components are shown, the submersible vehicle, the under ice base station, and the surface antenna. The base station and vehicle are deployed to the ocean through the borehole. The vehicle is able to acoustically communicate with the base station which can then be relayed through the surface antenna to Earth. Figure reproduced from (Branch et al. 2020). © 2020 IEEE.

Copyright © 2020 California Institute of Technology. Government sponsorship acknowledged.

Related Work

Traditional AUV navigation involves dead reckoning updated periodically with absolute positioning information such as GPS, Ultrashort Baseline (USBL), Long Baseline (LBL), or Short Baseline (SBL) navigation. With our constraints these methods of absolute positioning are not feasible.

USBL uses a single source and a single receiver with multiple transducers to determine the range and bearing of the receiver with respect to the source based on the phase shift between the transducers (Vickery 1998). This method requires high-frequency acoustics due to the small distance between the transducers, limiting the distance at which it is functional to under about 10km (this varies drastically depending on environmental conditions) and subsequently limiting the distance which the submersible could travel from the base station.

LBL uses multiple sources and a single receiver to triangulate the receiver with respect to the sources (Vickery 1998). (Webster et al. 2015) and (Jakuba et al. 2008) used LBL methods for under-ice AUV navigation. The sources must be separated by some distance. Such a system on an Ocean World would require multiple boreholes through the ice shell or a system to deploy acoustic sources under the ice, increasing complexity and cost.

SBL is similar to LBL in that it uses multiple sources and a single receiver to triangulate the receiver with respect to the sources. However the sources are usually deployed over the side of a single ship, resulting is a short baseline between sensors (Vickery 1998). As with LBL this would require multiple boreholes through the ice shell or a system to deploy acoustic sources under the ice, increasing complexity and cost.

Single beacon range-only acoustic navigation is well studied. Foundational work is presented in (Scherbatyuk 1995), using least squares to estimate vehicle position from multiple ranges. (Baccou and Jouvencel 2003), (Baccou and Jouvencel 2002), and (Vaganay, Baccou, and Jouvencel 2000) use a nonlinear least squares fit to initialize an estimate of the vehicle position and an EKF to provide continuous position updates as it homes to the source. (McPhail and Pebody 2009) and (Hartsfield Jr 2005) uses an iterative approach utilizing nonlinear least squares fit to estimate course. (LaPointe 2006) uses multiple ranges from a single source along a dead reckoned track and nonlinear least squares fit to simulate ranging from multiple sources. (Webster et al. 2012) uses a centralized EKF, receiving both ship and AUV data to perform navigation with one way travel time ranges. All the above works assume an absolute heading measurement such as that from a magnetic compass is available. Without such a sensor the error of the estimate from the EKF can grow unbounded. Given current knowledge about Ocean Worlds it is not guaranteed that such a sensor would be possible. Our method of single beacon homing does not require absolute heading information, only sufficiently accurate relative heading information over short periods of time.

Golden Section Search

The goal of the homing method is to select a heading that minimizes the rate of change of the measured range over time (Δ range). Note that this is a minimization problem because Δ range is negative when the distance between the vehicle and the beacon is decreasing. Given fixed currents, the Δ range to the beacon with respect to heading if very close to a sine curve, containing one minimum. The Δ range for a heading can be estimated by following a transect on that heading for some distance. We can use a modified Golden Section Search (Kiefer 1953) to locate the heading with the minimum Δ range. This search operates by estimating Δ range on 3 headings defining a search interval to determine if the maximum is located inside or outside of the interval. If it is outside, the interval is moved by calculating Δ range on an additional heading outside this interval. If the maximum is located inside the interval, then the size of that interval is reduced by calculating Δ range on a heading inside the interval. This repeats until the interval size reaches some threshold.

This method only requires relative heading information and therefore does not require magnetic navigation. Note that the function describing the Δ range to the beacon with respect to heading is time varying as the vehicle moves relative to the beacon and as currents change. In addition, the lack of an absolute heading will result in deviation from any commanded heading. We assume that the vehicle is able to maintain some heading and move between relative headings with enough accuracy to estimate the Δ range before errors render it invalid. This algorithm contains 3 main components. The next heading to probe is calculated from the current search interval, the vehicle is commanded along this heading to estimate the Δ range, then the search interval is updated based on the newly calculated Δ range.

Given an interval containing 0 to 3 Δ ranges calculated for some heading we can then calculate the next heading to probe. Given 3 headings, h_0, h_1, h_2, the following ratio must be maintained $(h_1 - h_0)/(h_2 - h_1) = \phi$, where ϕ is the golden ratio. Using this ratio insures that the next interval will be the same size independent of the specific interval selected. If the potential next intervals were not of the same size then bad luck could result in the larger interval being selected repeatedly, slowing convergence. The selection of the next heading is described in the GET_NEXT_HEADING procedure in Algorithm 1 and shown in Figure 2. GET_NEXT_HEADING takes two arguments, the list of headings on the interval, $headings$, and the Δ ranges for those headings, $delta\_ranges$. When the algorithm begins, these lists will be empty as no Δ ranges have been calculated. The first three probes, when the length of $headings$ is 0, 1, and 2, initialize the search interval. The first probe is some arbitrary heading, the second probe heading is offset $start\_interval/\phi$ from the first, and the third probe is selected such that it is adjacent to the minimum Δ range so far and offset by $start\_interval - (start\_interval/\phi)$ so the total interval size is equal to $start\_interval$ and the previously discussed ratio is preserved. For all subsequent heading selections, we will have 3 headings and Δ ranges that will dictate the next heading,

Copyright © 2020 California Institute of Technology. Government sponsorship acknowledged.

h_3. Without loss of generality, assume h_0, h_1, and h_2 form an interval in that order. There are 4 possible cases, however 2 are mirrored, so we will only discuss 2 cases here. Case 1: the minimum Δ range value of the current interval is on the right end of the interval, when $argmin(delta\_ranges)$ is 2. In this instance the next heading is selected outside of the current interval next to the current observed minimum. The probe selection point is $h_3 = h_2 + (h_1 - h_0)$. In this case the size of the interval does not change, however the interval is shifted towards the minimum. Note that the distance between h_2 and h_3 is equal to the distance between h_0 and h_1 to preserve the required ratio. The mirror of this case is when the minimum Δ range value is on the left end of the interval. Case 2: the minimum value of the current interval is in the middle of that interval and $h_1 - h_0 < h_2 - h_1$. In this instance the next heading is selected inside of the current interval, specifically between h_1 and h_2 as this gap is larger than between h_0 and h_1. To insure that the golden ratio is maintained and to place the next heading between h_1 and h_2, the selected heading should be $h_3 = h_0 + (h_2 - h_0)/\phi$. The mirror of this case is when $h_1 - h_0 > h_2 - h_1$.

Once the next heading is selected we must measure the Δ range over time along this heading. This is done by following a single heading while receiving multiple range distances. This is outlined in the MEASURE_DELTA_RANGE procedure in Algorithm 1. The vehicle is commanded along a specific heading. When the vehicle receives a new range, new_range, it recalculates the slope, new_slope, of all received ranges on this heading so far. This repeats until the end condition for following the heading is satisfied. This end condition is as follows. The standard deviation of the last $num\_slopes\_std\_dev$ slopes are calculated. The calculation of Δ range along this heading is considered complete when this standard deviation is below a specified value, $target\_slope\_std\_dev$, indicating that the calculated slope has stabilized with new range measurements. This will only occur after a minimum number of ranges are received to calculate the required standard deviation. If at any time during this process the vehicle has travelled along the given heading for $max\_time\_on\_transect$ seconds, then the Δ range calculation is completed and the latest slope is used.

Finally, we must update the current search interval. We have 4 Δ ranges on 4 headings and must down-select to 3. If the minimum Δ range is on the end of the interval then we take that heading and the two closest headings to it as the interval. If the minimum Δ range is in the middle of the interval then we take that heading and the two headings on either side of it as the interval. This is shown in Figure 3. We then repeat the heading selection, measurement, interval update processes until a given interval size has been reached. Once the given interval size has been reached we transition to following the heading that resulted in the minimum Δ range over time.

We follow this heading, continuing to measure the Δ range over time via a running average. When this decreases below a given percentage of the originally measured value we restart the Golden Section Search process. This repeats until we are within the target distance of the beacon.

Algorithm 1 Golden Section Search Homing

procedure GOLDEN_SECTION_SEARCH
  $headings \leftarrow$ empty list
  $delta\_range \leftarrow$ empty list
  while $headings.length < 3$ or
      $abs(heading[0] - heading[2]) > stop\_interval$ **do**
    $next\_heading \leftarrow get\_next\_heading(headings, delta\_ranges)$
    $change\_in\_range \leftarrow measure\_delta\_range(next\_heading)$
    append $next\_heading$ to $headings$
    append $change\_in\_range$ to $delta\_range$
    Sort $headings$ and $delta\_range$ based on $headings$
    if $headings.length == 4$ **then**
      if $argmax(delta\_range) == 0$ or $argmax(delta\_range) == 1$ **then**
        remove last entry in $headings$
        remove last entry in $delta\_range$
      else
        remove first entry in $headings$
        remove first entry in $delta\_range$
procedure GET_NEXT_HEADING(headings, delta_ranges)
  if headings.length == 0 **then**
    return 0
  else if headings.length == 1 **then**
    return $headings[0] + start\_interval/golden\_ratio$
  else if headings.length == 2 **then**
    if $argmin(delta\_ranges) == 0$ **then**
      return $headings[0] -$
          $(start\_interval - (start\_interval/golden\_ratio))$
    else if $argmin(delta\_ranges) == 1$ **then**
      return $headings[1] +$
          $(start\_interval - (start\_interval/golden\_ratio))$
  else if headings.length == 3 **then**
    if $argmin(delta\_ranges) == 0$ **then**
      return $heading[0] - abs(heading[1] - heading[2])$
    else if $argmin(delta\_ranges) == 1$ **then**
      if $heading[1] - heading[0] <$
          $heading[2] - heading[1]$ **then**
        return $heading[0] + abs(heading[0] - heading[2])/golden\_ratio$
      else
        return $heading[2] - abs(heading[0] - heading[2])/golden\_ratio$
    else if $argmin(delta\_ranges) == 2$ **then**
      return $heading[2] + abs(heading[0] - heading[1])$
procedure MEASURE_DELTA_RANGE(heading)
  Command vehicle along $next\_heading$
  $times \leftarrow$ empty list
  $ranges \leftarrow$ empty list
  $slopes \leftarrow$ empty list
  do
    Wait for next range
    append new_range to $ranges$
    append new_range_time to $times$
    $new\_slope \leftarrow least\_squares\_slope(times, ranges)$
    append new_slope to $slopes$
    if $slopes.length > num\_slopes\_std\_dev$ **then**
      remove first entry in $slopes$
  while time on transect $< max\_time\_on\_transect$ and
      ($slopes.length < num\_slopes\_std\_dev$ or
       std dev of $slopes > target\_slope\_std\_dev$)
  return Last entry in $slopes$

Copyright © 2020 California Institute of Technology. Government sponsorship acknowledged.

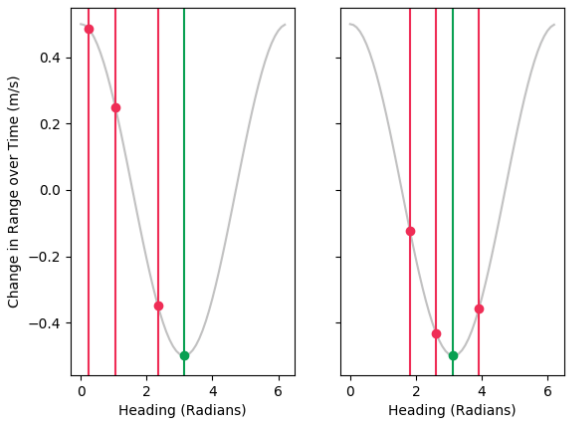

Figure 2: Plot describing the process of selecting the next heading for Golden Section Search. The function describing Δ range is shown in light grey, heading is plotted along the x axis and Δ range over time on the y axis. The current interval is shown in red, with lines at each heading and a dot at the measured value. The next heading selected is shown in green. Two of the four cases are shown. The remaining two cases are mirrored.

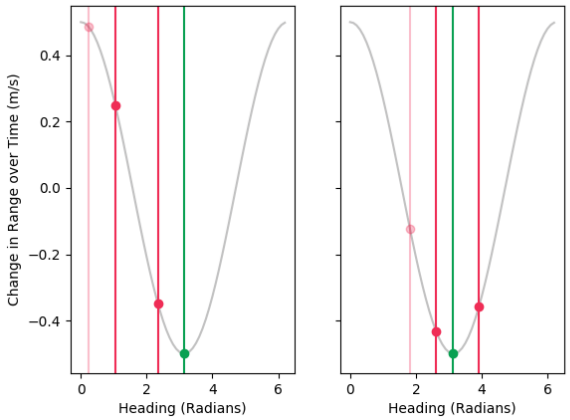

Figure 3: Plot describing the process of selecting the new interval given the old interval and a new measurement. The function describing Δ range is shown in light grey, heading is plotted along the x axis and Δ range over time on the y axis. The current interval is shown in red, with lines at each heading and a dot at the measured value. The new measurement is shown in green. The new interval is the three saturated lines. The faded red line is removed from the interval. Two of the four cases are shown. The remaining two cases are mirrored.

Simulation Experiment

All experiments are performed in a simulation environment. An FVCOM (Chen, Liu, and Beardsley 2003) based ocean circulation model of Axial Seamount on the Juan de Fuca Ridge is used to provide realistic currents. X-Y resolution is 200m at the model center with resolution decreasing outwards. There are 127 Z layers uniformly distributed between the surface and the seafloor at any given location, providing approximately 12-20m of resolution in our operation region. Outputs from the HYbrid Coordinate Ocean Model (HYCOM), OSU Tidal Inversion, and the National Centers for Environmental Prediction (NCEP) Climate Forecast System Reanalysis (CFSR) are incorporated into the FVCOM model used.

The simulated AUV is equipped with an IMU and an acoustic receiver. The angular velocity measurements provided by the IMU along with the commanded target velocity are used in a simple dead reckoning system. Note that we do not use any absolute heading measurements. We use a simple error model for both sensors. Random Gaussian error and a fixed bias are introduced into the range measurements from the acoustic beacon and the angular velocity measurements. The bias and standard deviation of the range error is determined as a percentage of the true range measurement, so smaller ranges have smaller bias and errors. Angular velocity measurements use a fixed bias and standard deviation in degrees/s.

Ranges are provided to the vehicle once every 60 seconds. The vehicle has a target X-Y velocity of 0.5 m/s and maintains a fixed depth. Four locations for the base station are used in the model to allow for different current profiles. For each base station location and parameter permutation there are 8 runs. In these 8 runs the vehicle starts 10 km away from the base station at 45 degree intervals. The first heading of the Golden Section Search algorithm is always 0 degrees. Success is declared when the vehicle reaches acoustic communication range, 1 km in our experiments. If 48 hours pass and the vehicle is unable to come within this range it is considered a failure. In 48 hours the vehicle can travel approximately 86.4 km. We varied the error parameters for the simulated acoustic and IMU sensors. A single error parameter is varied at a time, while the remaining error parameters remain fixed. The fixed error parameters are as follows: range standard deviation = 5%, range bias = 5%, angular velocity standard deviation = 0.25 degrees/s, angular velocity bias = 0.005 degrees/s.

Results

A set of example runs can be seen in Figure 4. In this example we see better performance from (a) where the algorithm is able to more accurately determine the direction of the beacon relative to the vehicle, taking a more direct path and needing to restart the search less frequently.

Figure 5 and Figure 6 show the performance of the algorithm as the quality of the range and angular velocity measurements decrease respectively. For each plot, the x axis is one of the four error parameters. The percent of runs that were successful is shown in red, corresponding to the right y-axis. The total distance travelled of each individual run is shown as a blue point with the average as a blue line, corresponding to the left y-axis. The error parameters are standard deviation of the random Gaussian error and fixed bias for the

Copyright © 2020 California Institute of Technology. Government sponsorship acknowledged.

range and angular velocity measurements. The range and angular velocity error parameters are measured as a percentage of the true range and as degrees/s, respectively. The minimum distance travelled to end within 1 km of the beacon is 9 km, the approximate maximum distance before failure is 86.4 km (based on the vehicles target horizontal speed). As most error parameters increase we see a sharp decrease in the number of successful runs. We also see a rise in the average and variance of the distance travelled to achieve success. The one exception to this is the range fixed bias.

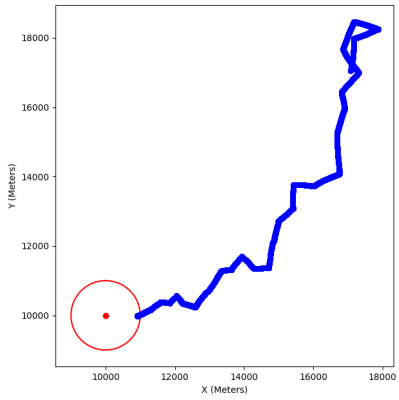

(a)

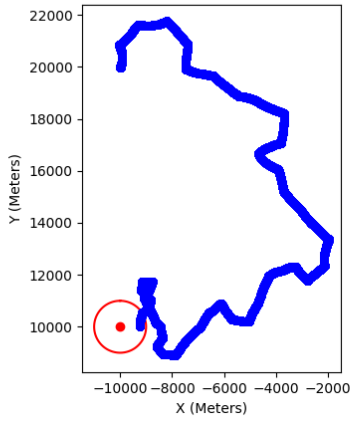

(b)

Figure 4: Two successful example runs. The vehicle path is shown in blue with the starting location towards the top of each plot. The acoustic beacon location is shown as a red point and the 1km target range is shown as a red ring. The run in the top figure has parameters: range standard deviation = 5%, range bias = 5%, angular velocity standard deviation = 0.25 degrees/s, angular velocity bias = 0.005 degrees/s. The run in the bottom figure has parameters: range standard deviation = 10%, range bias = 5%; angular velocity standard deviation = 0.4 degrees/s, angular velocity bias = 0.005 degrees/s.

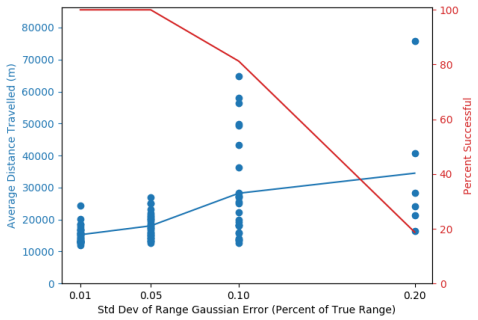

(a)

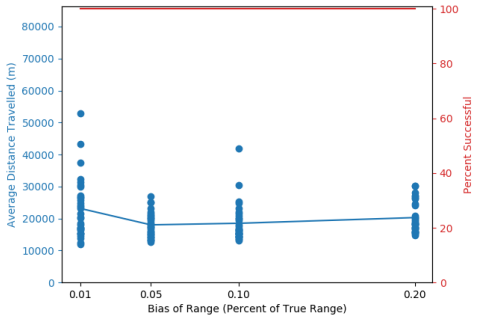

(b)

Figure 5: Plots showing the performance of the algorithm against the error parameters of ranges. Plot (a) varies the standard deviation of the Gaussian error and plot (b) varies the bias of the range measurements. All other error parameters are fixed. The blue dots shows the average distance travelled to achieve success from a single run, with 32 runs per parameter value. The blue line shows the average of all runs. The red line shows the percentage of runs that were successful. These correspond to the left (blue) and right (red) y-axis respectively.

Discussion

The viability of this method depends on the error characteristics of the internal navigation sensors and ranging capabilities of the vehicle. By increasing the error of range and angular velocity measurements the average required time and distance travelled to home to the base station significantly increased, as did the uncertainty of these metrics. The one exception to this is the range bias. As the range bias is fixed and we only need the relative ranges over a short period of time, this has little effect on the ability to estimate Δ range over time.

The dead reckoning and ranging capabilities of the vehicle are both critical to the calculation of Δ range on a specific heading. An increase in the number of ranges taken or reduced error of those ranges will require the vehicle to maintain a heading for a shorter time interval, therefore reducing error introduced by the dead reckoning system. Additional ranging measurements would come at the cost of increased power consumption at the base station. On the other hand,

Copyright © 2020 California Institute of Technology. Government sponsorship acknowledged.

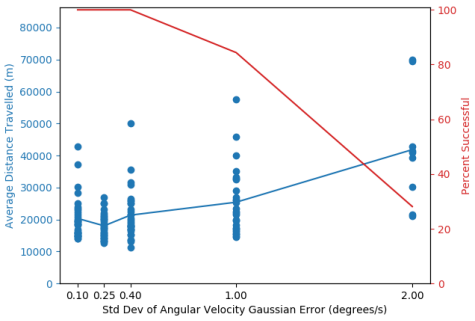

(a)

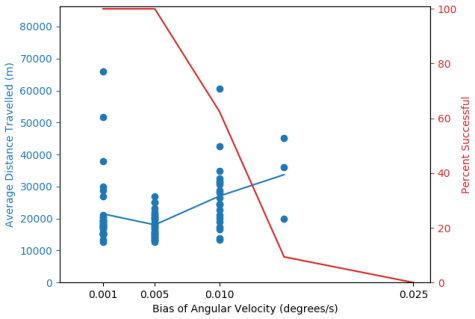

(b)

Figure 6: Plots showing the performance of the algorithm against the error parameters of the angular velocity measurement. Plot (a) varies the standard deviation of the Gaussian error and plot (b) varies the bias of the angular velocity measurements. All other error parameters are fixed. The blue dots shows the average distance travelled to achieve success from a single run, with 32 runs per parameter value. The blue line shows the average of all runs. The red line shows the percentage of runs that were successful. These correspond to the left (blue) and right (red) y-axis respectively.

if the dead reckoning system is improved, then the vehicle can maintain a specific heading for a longer time. Allowing for more range measurements to be collected to compensate for more error in those ranges. The viability of this method would need to be analysed on a case-by-case basis given the requirements of a specific AUV and mission/field program.

Future Work

The next step is to demonstrate this in a field program onboard an AUV. While this initial simulation is promising, the fidelity at which we can simulate underwater acoustics, ocean currents, and sensor error characteristics is limited. Confidence in this homing algorithm can only be achieved through in-water testing. This method and any other navigation methods need to be integrated with a broader mission plan akin to that in (Thompson et al. 2017), incorporating autonomous science capabilities such as ocean front and feature tracking (Branch et al. 2019; Zhang et al. 2016; Cruz and Matos 2014; Flexas et al. 2018).

We assume that false ranges are filtered. Previous work on filtering acoustic ranges for AUVs needs to be applied following the constraints presented here. This method needs to be tested in comparison to other single beacon homing and navigation techniques. This method covers the domain where the vehicle is distant from the base station, but still in range of the acoustic beacon for ranging. Two additional domains need to be handled, when the vehicle is close to the base station and requires fine-grain navigation and when the vehicle loses contact with or is out of range of the acoustic beacon. This method provides homing capabilities, however vehicle localization is not possible. To maximize science return of an Ocean Worlds submersible, vehicle navigation would be required to locate data and revisit regions of interest.

Conclusion

We demonstrated a method for AUV homing using a single range-only acoustic beacon and no absolute heading information. This method was tested using a simulated vehicle, sensors, and realistic currents. We show that this method is capable of homing from 10km to within 1km of an acoustic beacon, with various amounts of sensor error.

Acknowledgments

The research was carried out at the Jet Propulsion Laboratory, California Institute of Technology, under a contract with the National Aeronautics and Space Administration (80NM0018D0004).

References

Baccou, P., and Jouvencel, B. 2002. Homing and navigation using one transponder for auv, postprocessing comparisons results with long base-line navigation. In *Proceedings 2002 IEEE International Conference on Robotics and Automation (Cat. No. 02CH37292)*, volume 4, 4004–4009. IEEE.

Baccou, P., and Jouvencel, B. 2003. Simulation results, postprocessing experimentations and comparisons results for navigation, homing and multiple vehicles operations with a new positioning method using on transponder. In *Proceedings 2003 IEEE/RSJ International Conference on Intelligent Robots and Systems (IROS 2003)(Cat. No. 03CH37453)*, volume 1, 811–817. IEEE.

Branch, A.; Flexas, M. M.; Claus, B.; Thompson, A. F.; Zhang, Y.; Clark, E. B.; Chien, S.; Fratantoni, D. M.; Kinsey, J. C.; Hobson, B.; et al. 2019. Front delineation and tracking with multiple underwater vehicles. *Journal of Field Robotics* 36(3):568–586.

Branch, A.; McMahon, J.; Xu, G.; Jakuba, M. V.; German, C. R.; Chien, S.; Kinsey, J. C.; Bowen, A. D.; Hand, K. P.; and Seewald, J. S. 2020. Demonstration of autonomous nested search for local maxima using an unmanned underwater vehicle. In *International Conference on Robotics and Automation (ICRA 2020)*.

Chen, C.; Liu, H.; and Beardsley, R. C. 2003. An unstructured grid, finite-volume, three-dimensional, primitive

Copyright © 2020 California Institute of Technology. Government sponsorship acknowledged.

REFERENCES

equations ocean model: Application to coastal ocean and estuaries. *Journal of Atmospheric and Oceanic Technology* 20(1):159–186.

Cruz, N. A., and Matos, A. C. 2014. Autonomous tracking of a horizontal boundary. In *Oceans-St. John's, 2014*, 1–6. IEEE.

Flexas, M. M.; Troesch, M. I.; Chien, S.; Thompson, A. F.; Chu, S.; Branch, A.; Farrara, J. D.; and Chao, Y. 2018. Autonomous sampling of ocean submesoscale fronts with ocean gliders and numerical model forecasting. *Journal of Atmospheric and Oceanic Technology* 35(3):503–521.

Hartsfield Jr, J. 2005. Single transponder range only navigation geometry (strong) applied to remus autonomous under water vehicles. Technical report, Massachusetts Inst of Tech Cambridge.

Jakuba, M. V.; Roman, C. N.; Singh, H.; Murphy, C.; Kunz, C.; Willis, C.; Sato, T.; and Sohn, R. A. 2008. Long-baseline acoustic navigation for under-ice autonomous underwater vehicle operations. *Journal of Field Robotics* 25(11-12):861–879.

Kiefer, J. 1953. Sequential minimax search for a maximum. *Proceedings of the American mathematical society* 4(3):502–506.

LaPointe, C. E. 2006. Virtual long baseline (vlbl) autonomous underwater vehicle navigation using a single transponder. Technical report, Massachusetts Inst of Tech Cambridge.

McPhail, S. D., and Pebody, M. 2009. Range-only positioning of a deep-diving autonomous underwater vehicle from a surface ship. *IEEE Journal of Oceanic Engineering* 34(4):669–677.

National Aeronautics and Space Administration. 2018. Ocean worlds.

Scherbatyuk, A. P. 1995. The auv positioning using ranges from one transponder lbl. In *'Challenges of Our Changing Global Environment'. Conference Proceedings. OCEANS'95 MTS/IEEE*, volume 3, 1620–1623. IEEE.

Thompson, A. F.; Chao, Y.; Chien, S.; Kinsey, J.; Flexas, M. M.; Erickson, Z. K.; Farrara, J.; Fratantoni, D.; Branch, A.; Chu, S.; Troesch, M.; Claus, B.; and Kepper, J. 2017. Satellites to seafloor: Toward fully autonomous ocean sampling. *Oceanography* 30(2):160–168.

Vaganay, J.; Baccou, P.; and Jouvencel, B. 2000. Homing by acoustic ranging to a single beacon. In *OCEANS 2000 MTS/IEEE Conference and Exhibition. Conference Proceedings (Cat. No. 00CH37158)*, volume 2, 1457–1462. IEEE.

Vickery, K. 1998. Acoustic positioning systems. a practical overview of current systems. In *Proceedings of the 1998 Workshop on Autonomous Underwater Vehicles (Cat. No. 98CH36290)*, 5–17. IEEE.

Webster, S. E.; Eustice, R. M.; Singh, H.; and Whitcomb, L. L. 2012. Advances in single-beacon one-way-travel-time acoustic navigation for underwater vehicles. *The International Journal of Robotics Research* 31(8):935–950.

Webster, S. E.; Freitag, L. E.; Lee, C. M.; and Gobat, J. I. 2015. Towards real-time under-ice acoustic navigation at mesoscale ranges. In *2015 IEEE International Conference on Robotics and Automation (ICRA)*, 537–544. IEEE.

Zhang, Y.; Bellingham, J. G.; Ryan, J. P.; Kieft, B.; and Stanway, M. J. 2016. Autonomous four-dimensional mapping and tracking of a coastal upwelling front by an autonomous underwater vehicle. *Journal of Field Robotics* 33(1):67–81.

Copyright © 2020 California Institute of Technology. Government sponsorship acknowledged.